

Lower limit to the thermal conductivity of disordered crystals

David G. Cahill

Department of Materials Science and Engineering, University of Illinois, Urbana, Illinois 61801

S. K. Watson and R. O. Pohl

Laboratory of Atomic and Solid State Physics, Cornell University, Ithaca, New York 14853-2501

(Received 3 February 1992)

Measurements of the thermal conductivity above 30 K of mixed crystals with controlled disorder, $(\text{KBr})_{1-x}(\text{KCN})_x$, $(\text{NaCl})_{1-x}(\text{NaCN})_x$, $\text{Zr}_{1-x}\text{Y}_x\text{O}_{2-x/2}$, and $\text{Ba}_{1-x}\text{La}_x\text{F}_{2+x}$, support the idea of a lower limit to the thermal conductivity of disordered solids. In each case, as x is increased, the data approach the calculated minimum conductivity based on a model originally due to Einstein. These measurements support the claim that the lattice vibrations of these disordered crystals are essentially the same as those of an amorphous solid.

I. INTRODUCTION

We have shown previously^{1,2} that the thermal conductivity of amorphous solids above ~ 30 K can be described with a model originally proposed by Einstein³ who assumed that the mechanism of heat transport in crystals was a random walk of the thermal energy between neighboring atoms vibrating with random phases.² In Ref. 2, we also stated that the same model applies to a number of highly disordered crystals, and that we have never been able to produce a disordered crystal with a thermal conductivity smaller than the prediction of the model. This latter observation encouraged us to refer to Einstein's model as that of the *minimum thermal conductivity*, a concept first proposed by Slack.⁴

Heat transport in disordered materials has been the subject of several recent theoretical investigations. For a review of the fracton model with comparison to thermal-conductivity data for amorphous solids, see Ref. 5. Allen and Feldman⁶ calculated the thermal conductivity of α -Si using a harmonic, Kubo-Greenwood approach and found good agreement with experimental data⁷ near room temperature. Molecular dynamics calculations^{8,9} are also in good agreement with the data.

Naturally occurring disordered crystals with low, glasslike thermal conductivities were studied by Birch and Clark¹⁰ in their work on the thermal conductivity of feldspar minerals above room temperature. Some feldspar minerals have a thermal conductivity that is remarkably similar to an amorphous solid over the entire temperature range of $0.1 < T < 300$ K, as illustrated in Fig. 1. Unfortunately, unraveling the cause of the low conductivity has been complicated by the complex crystal structure and growth conditions of naturally occurring minerals.

Many types of disordered crystals have been shown to have glasslike thermal conductivities:^{11,12} Bi_2O_3 ,¹³ the so-called dirty ferroelectrics,¹⁴ certain glass ceramics,¹⁵ and YB_{66} ,¹⁶ to mention a few examples. As in the case

of the feldspars, the experimentalist has little control over the degree or type of disorder present in these crystals.

Experiments on structurally simple crystals with disorder that can be systematically controlled allow us to demonstrate more clearly the validity of Einstein's model and the concept of a minimum thermal conductivity. For example, the mixed crystal $(\text{KBr})_{1-x}(\text{KCN})_x$ can be made for any value of x and near $x = 0.50$ the thermal conductivity and low-temperature specific heat are glasslike.²⁶ To help elucidate the types of disorder that can produce a glasslike conductivity, we have extended previous low-temperature measurements of the thermal

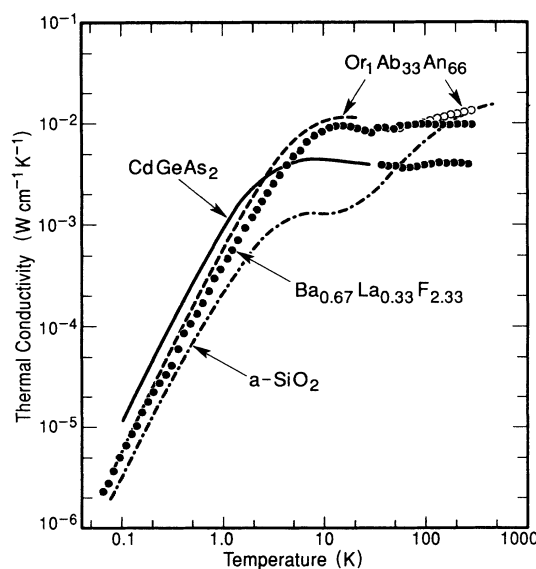


FIG. 1. Data for two disordered single crystals with glasslike thermal conductivity: $\text{Or}_1\text{Ab}_{33}\text{An}_{66}$ feldspar and $\text{Ba}_{1-x}\text{La}_x\text{F}_{2+x}$, $x = 0.33$ compared to data for two amorphous solids: α - SiO_2 and CdGeAs_2 . Data for feldspar below 30 K are from Ref. 30.

conductivity of a number of other disordered crystals to room temperature. One system of mixed crystals, $\text{Ba}_{1-x}\text{La}_x\text{F}_{2+x}$ discussed below, provides a structurally simple example of a crystal with glasslike conductivity;²⁸ see Fig. 1.

In this paper, we present detailed measurements of these disordered crystals and explore structural similarities. Low-temperature measurements for most of these crystals have been published previously; for the sake of completeness, these data are included. The paper begins with a detailed presentation of Einstein's arguments on which the model is based.

II. EINSTEIN'S MODEL

In 1911, Einstein published³ his calculation of the thermal conductivity of solids in an attempt at understanding recent thermal conductivity data of Eucken¹⁷ on crystalline solids between 80 and 373 K. The calculation was an extension of his successful theory for the specific heat of solids.¹⁸

Since Einstein's paper is not readily available to most researchers and has not been, to our knowledge, translated into English, we reproduce his arguments below. This is not a direct translation of Einstein's paper, but his notation has been maintained.

Einstein started from his 1907 model for the atomic vibrations of a solid as harmonic oscillators, all vibrating at the same frequency ν .¹⁸ If the oscillators are not coupled to one another, the thermal conductivity of this model solid is zero: thermal energy cannot be transmitted from one atom to another. For thermal transport to occur, the oscillators must be coupled, and Einstein did this by supposing that each atom was connected to its neighbors on a simple-cubic lattice by harmonic forces. Einstein chose to couple each oscillator to its first-, second-, and third-nearest neighbors (6+12+8, a total of 26) to maximize the heat flow.

The angles and distances between a central atom M

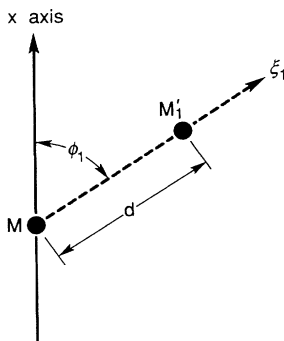


FIG. 2. Description of angles and displacements in Einstein's calculation of the thermal conductivity of solids. The oscillatory displacements x and ξ_1 are small relative to the interatomic spacing d .

and one of its neighbors M'_1 are shown in Fig. 2. Atom M moves in the x direction and is displaced from its equilibrium position by a distance x under the influence of the force exerted by M on M'_1 . Atom M'_1 moves in the direction of M to M'_1 and is displaced from its equilibrium position by a distance ξ_1 . The equilibrium separation of the two atoms is d , which is large in comparison to the displacements x and ξ_1 . The direction from M to M'_1 makes an angle φ_1 with the x axis. Using a as the force constant of the spring that connects M and M'_1 , the force on atom M in the x direction is

$$a(\xi_1 - x \cos \varphi_1) \cos \varphi_1 . \quad (1)$$

With m as the mass of atom M , the x component of the equation of motion for M is

$$m \frac{d^2 x}{dt^2} = -ax \sum_n \cos^2 \varphi_n + \sum_n a \xi_n \cos \varphi_n , \quad (2)$$

where the sum is over all 26 neighbors.

As shown below, the oscillators do not oscillate sinusoidally about their equilibrium positions, but it is a reasonable approximation to assume so at this point:

$$x = A \sin 2\pi\nu t , \quad (3)$$

$$\xi_n = A'_n \sin(2\pi\nu t + \alpha_n) , \quad (4)$$

with the crucial assumption that α_n is a random phase difference, i.e., there is no coherence between the motions of neighboring atoms. This is the fundamental difference between Einstein's model and the models of Debye and of Born and von Karman.

Multiplying Eq. (2) by $(dx/dt)dt$ and integrating with respect to time gives an equation in the energy of atom M :

$$\int d \left\{ m \frac{\dot{x}^2}{2} + \sum_n (a \cos^2 \varphi_n) \frac{x^2}{2} \right\} = \sum_n a \cos \varphi_n \int \xi_n \frac{dx}{dt} dt . \quad (5)$$

Equation (5) expresses the changes Δ in the energy of atom M as a result of the work η_n done by neighboring atoms M'_n :

$$\Delta = \sum_n \eta_n , \quad (6)$$

where

$$\eta_n = a \cos \varphi_n \int \xi_n \frac{dx}{dt} dt . \quad (7)$$

Inserting Eqs. (3) and (4) for x and ξ_n and integrating Eq. (7) over one half a period of oscillation, one obtains

$$\eta_n = \frac{\pi}{2} a A A'_n \cos \varphi_n \sin \alpha_n . \quad (8)$$

Since α_n is a random variable, there are just as many neighbors that add as subtract energy from atom M .

The average change in the energy of M is zero, $\overline{\Delta} = 0$. The mean-square fluctuations $\overline{\Delta^2}$, however, are nonzero:

$$\overline{\Delta^2} = \sum_n \overline{\eta_n^2} , \quad (9)$$

where the average is over different time intervals of one half a period of oscillation, and the average was moved inside the summation, since the η_n are uncorrelated.

From Eq. (8),

$$\overline{A^2 A_n'^2 \sin^2 \alpha_n} = \frac{1}{2} \overline{A^2}^2 , \quad (10)$$

so that

$$\overline{\eta_n^2} = \left(\frac{\pi}{2}a\right)^2 \frac{1}{2} \overline{A^2}^2 \cos^2 \varphi_n \quad (11)$$

and

$$\overline{\Delta^2} = \frac{\pi^2}{8} a^2 \overline{A^2}^2 \sum_n \cos^2 \varphi_n . \quad (12)$$

A reasonable estimate of the last sum gives $\sum_n \cos^2 \varphi_n = 10$, and taking the square root of each side,

$$\sqrt{\overline{\Delta^2}} = \sqrt{\frac{10}{8}} \pi a \overline{A^2} . \quad (13)$$

We can now compare the root-mean-square energy fluctuations of atom M to its average potential energy. The potential energy of atom M displaced from equilibrium by a distance x is

$$a \frac{x^2}{2} \sum_n \cos^2 \varphi_n = a \frac{x^2}{2} 10 , \quad (14)$$

and the average potential energy is

$$5a \overline{x^2} = \frac{5}{2} a \overline{A^2} . \quad (15)$$

The average total energy is just twice the average potential energy:

$$\overline{E} = 5a \overline{A^2} . \quad (16)$$

By comparing this last result with Eq. (13), we see that the average of the energy fluctuations $\sqrt{\overline{\Delta^2}}$ is comparable to the average energy \overline{E} . If the actual motion of atoms were used instead of the assumed sinusoidal motion, Eqs. (3) and (4), the conclusion would be the same. Following Einstein, we interpret this result to mean that the thermal energy of each atom is lost (or gained) during one half a period of oscillation of the atom.

In order to add temperature dependence to his model, Einstein proposed that the oscillators were quantized and therefore the specific heat of this model solid would decrease with decreasing temperature. Einstein found that his model failed to reproduce not only the temperature dependence, but also the absolute magnitude of the thermal conductivity of crystals. As pointed out by Debye and by Born and von Karman, the periodicity of a crystalline lattice produces coherence between the atomic oscillators, and therefore, Einstein's assumption

of a random phase between oscillators was flawed. However, his model does appear to apply to amorphous solids and certain highly disordered crystals, as we reported previously.^{1,2}

To remove the uncertainty of choosing the Einstein frequency, we modified Einstein's result somewhat in our previous work by including larger oscillating entities than the single atoms considered by Einstein. For this, we borrowed from the Debye model of lattice vibrations and divided the sample into regions of size $\lambda/2$, whose frequencies of oscillation are given by the low-frequency speed of sound $\omega = 2\pi v/\lambda$. The lifetime of each oscillator was again assumed to be one half the period of vibration, i.e., $\tau = \pi/\omega$. The thermal conductivity resulting from the random walk between these localized quantum mechanical oscillators can then be written as the following sum of three Debye integrals:²

$$\Lambda_{\min} = \left(\frac{\pi}{6}\right)^{1/3} k_B n^{2/3} \sum_i v_i \left(\frac{T}{\Theta_i}\right)^2 \int_0^{\Theta_i/T} \frac{x^3 e^x}{(e^x - 1)^2} dx . \quad (17)$$

The sum is taken over the three sound modes (two transverse and one longitudinal) with speeds of sound v_i ; Θ_i is the cutoff frequency for each polarization expressed in degrees K, $\Theta_i = v_i(\hbar/k_B)(6\pi^2 n)^{1/3}$, and n is the number density of atoms. We repeat, however, that our physical picture is that of a random walk of energy between localized oscillators of varying sizes and frequencies and that the dominant energy transport is between nearest neighbors. Equation (17) contains no free parameters, for v_i and n are known.

III. EXPERIMENTAL DETAILS

Data from 30 K to room temperature were obtained using the 3ω measurement technique.¹⁹ The 3ω method is an ac measurement technique that is insensitive to errors from black-body radiation. Also, this method does not suffer from the long equilibration times that complicate traditional dc measurements at elevated temperatures. The term 3ω refers to the third harmonic detection scheme we use to measure the self-heating of a narrow metal line.²⁰ We first became aware of the use of third harmonic detection of self-heating through the work of Birge and Nagel,^{21,22} who used a different geometry to measure the product of the thermal conductivity and the heat capacity.

A 3000-Å-thick film of Ag evaporated onto the sample serves as both the heater and thermometer²³ in these experiments. For the fluoride and oxide crystals described below, the Ag film was patterned into a narrow line, 0.035×4.0 mm, using photolithography. In the case of water soluble alkali halide and alkali cyanide crystals, the Ag line was produced directly by evaporation through a mask fashioned from the opposing edges of razor blades. In this case, the dimensions of the metal line were typically 0.08×6.0 mm. The thermal conductivity is determined from the frequency dependence of the self-heating of this metal line.¹⁹ The resistance of the Ag line be-

comes increasingly less sensitive to changes in temperature below 30 K, setting the lower limit to the useful temperature range of the 3ω method.

To prepare the samples for the 3ω measurements, alkali halide and cyanide crystals were cleaved along the $\langle 100 \rangle$ direction into a plate geometry, $1 \times 1 \times 0.2$ cm. We found that a light polish of the surface with fine alumina powder aided the adherence of the metal line to these samples. More effort was required for high-concentration cyanide crystals; after cleaving, the samples were coated with a dilute film of GE 7031 varnish to prevent corrosion of the metal line. Fluoride and oxide crystals were cut into the same plate geometry using a wire saw and then polished to a matte finish before depositing the metal film.

All data for disordered crystals were obtained on single crystals. The composition of the $\text{KCl}_{0.52}\text{Br}_{0.48}$ crystal is that of the melt and is from the same boule as studied by Karlsson.²⁴ The composition of $(\text{KBr})_{1-x}(\text{KCN})_x$ crystals was determined from density measurements as reviewed in Ref. 25. Some previous Cornell data for $(\text{KBr})_{1-x}(\text{KCN})_x$ crystals were reported using the concentrations of the melt; the sample referred to as $x = 0.25$ (in the melt) in Ref. 26 is referred to here as $x = 0.19$ (composition of the crystal).

The compositions of two $(\text{NaCl})_{1-x}(\text{NaCN})_x$ crystals were characterized by ir absorption. We determined that the cyanide concentration in the melt was twice as large as the concentration in the crystals for compositions $x = 0.025$ and 0.05 . A third crystal, also grown at Cornell with $x = 0.20$ in the melt was not characterized by ir absorption. Assuming the same rate of cyanide incorporation gives approximately $x \approx 0.10$ in this crystal; $x \approx 0.10$ is the value we will use in the following to refer to this crystal. A fourth crystal of composition $x = 0.76$ was obtained from K. Knorr who determined the concentration from a measurement of the lattice constant.²⁷

$\text{Ba}_{1-x}\text{La}_x\text{F}_{2+x}$ crystals were purchased from Optovac; La concentrations were determined from x-ray fluorescence data.²⁸ Samples with $x = 0.33$ and 0.46 were confirmed to have the fluorite structure by x-ray diffraction. The $x = 0.46$ sample was not measured below 30 K because it was not as high quality as the other samples; the $x = 0.46$ sample had a yellowish tint, while all the other samples were clear. However, low-temperature internal friction measurements showed identical Q^{-1} to that of the $x = 0.33$ sample²⁸ thus confirming the existence of low-energy excitations in the $x = 0.46$ sample.

$\text{Zr}_{1-x}\text{Y}_x\text{O}_{2-x/2}$ crystals, grown by a skull method, were provided by J. Smith²⁹ with compositions determined by chemical analysis.

The feldspars studied are natural crystals from a variety of sources. $\text{Ab}_{99}\text{An}_1$ is a low albite, kindly provided by Dr. H. Pentinghaus (Kernforschungszentrum Karlsruhe). The Al^{3+} and Si^{4+} ions are almost fully ordered as a result of its thermal history; however, (chemical) alterations led to internal scattering structures spaced by $\sim 50 \mu\text{m}$, which limit the conductivity below 10 K. The sample labeled $\text{Or}_{90}\text{Ab}_{10}$ is a clear gem-quality single-crystal orthoclase from Fianarntsoa,

Madagascar. The $\text{Or}_{86}\text{Ab}_{14}$ is a gem-quality clear single crystal (labeled Sanidine No. 1 in Ref. 30) from the Eiffel, kindly supplied by Dr. H. Wondratschek (Karlsruhe University). The single crystal $\text{Or}_{3.3}\text{Ab}_{48.7}\text{An}_{48}$ [composition determined by microprobe analysis by Dr. H.U. Nissen and Dr. R. Wessicken (ETH Zürich)] is a labradorite sample from Tabor Island, Nain, Labrador (labeled e-plagioclase No. 1 in Ref. 30). Because of its thermal history, it contained exsolution lamellae leading to schiller. This sample is similar to the labradorite measured previously,³¹ but contained fewer ilmenite inclusions, which in this earlier sample had led to enhanced low-temperature phonon scattering. The optically clear, single crystal $\text{Or}_1\text{Ab}_{33}\text{An}_{66}$ labradorite came from Sage Brush Flat, Warner Valley, Lake County, Oregon (b-plagioclase in Ref. 30). It is volcanic in origin, cooled relatively rapidly, and therefore does not contain composition modulations, in contrast to the e-plagioclase No. 1. The $\text{Ab}_{50}\text{An}_{50}$ is a glass produced by Dr. Pentinghaus.

IV. RESULTS AND DISCUSSION

A. Mixed alkali halides and cyanides

Some of the simplest mixed crystals are mixtures of alkali halides. For example, $\text{KCl}_{1-x}\text{Br}_x$ can be grown as a single crystal for all values of x . The Br^- ion substitutes for the Cl^- ion in the sodium chloride structure. This system was the subject of one of the first studies of the effects of disorder on thermal conductivity.³² Baumann and Pohl³³ studied $\text{KCl}_{1-x}\text{Br}_x$ for the effects of monatomic impurities on the conductivity and were able to explain their data using a combination of Rayleigh and impurity mode scattering: the strength of the Rayleigh scattering and the frequency of the impurity mode agree with simple models based on mass mismatch alone. While substitution of Br for Cl reduces the conductivity significantly, a glasslike value is not reached even at the highest level of disorder $x \approx 0.50$; see Fig. 3. The type of disorder in $\text{KCl}_{1-x}\text{Br}_x$, substitution with an ion of the same charge, even one with a large mass difference, does not lead to a glasslike conductivity at any temperature.

This is also true for $\text{KBr}_{1-x}\text{I}_x$ as studied by Nathan, Lou, and Tait.³⁴ The situation is more complicated because $\text{KBr}_{1-x}\text{I}_x$ does not form a single crystal near $x = 0.50$ and phase separates into crystallites of varying composition. However, the conductivity near $x = 0.5$ is similar to $\text{KCl}_{1-x}\text{Br}_x$, $x = 0.5$ and again greatly exceeds the glasslike magnitude at all temperatures.

Further confirmation that simple, monatomic substitution cannot produce glasslike conductivities, comes from data on mixed crystals outside of the family of alkali halides. For example, the thermal conductivity of Si-Ge alloys³⁵ exceeds the minimum conductivity by more than an order of magnitude at room temperature for all compositions. Below, we will describe another example of monatomic substitution in the fluorite structure crystals.

In contrast to monatomic crystalline mixtures, mixtures of alkali halides with cyanides can produce a

glasslike conductivity; $(\text{KBr})_{1-x}(\text{KCN})_x$ is the most thoroughly studied example. Each CN^- molecule substitutes for a Br^- ion with only a small change in the volume of the unit cell. As a result, single crystals can be grown for any value of x (as long as the starting melt is of high purity) and this was the first mixed crystal to fully demonstrate the evolution of glasslike thermal properties in a disordered crystal.²⁶

In Fig. 4, we show our high temperature data for a crystal with $x = 0.19$ and 0.41 plotted with low-temperature ($T < 30$ K) data by De Yoreo *et al.*³⁶ De Yoreo *et al.* also measured the conductivity between 30 and 100 K and observed a jump in the conductivity of $x = 0.19$ near 70 K. The temperature of this jump shifted when the same sample was remounted in the cryostat. To check this result, we took data while cooling from 300 to 30 K and while heating back to 300 K using the 3ω method and obtained the same smooth curve both times; see Fig. 4. The earlier data³⁶ were probably in error and illustrate the serious difficulties (black-body radiation and long equilibration

times) encountered in measuring poor conductors at high temperatures using the standard technique.

The conductivity of $(\text{KBr})_{1-x}(\text{KCN})_x$, $x = 0.19$ and $x = 0.41$, is glasslike at all temperatures and approaches the calculated Λ_{\min} near room temperature; see Fig. 4. Perhaps this is due to the extra degree of freedom, librational motion, of the CN molecule compared to the Br ion it replaces. Grannan, Randeria, and Sethna³⁷ showed that if these librations are strongly coupled to phonons, they can produce phonon scattering large enough to explain the plateau region (2–100 K) in the thermal conductivity. Presumably, the phonon scattering is also strong enough near room temperature to produce lattice vibrations much like those of glasses.

The $(\text{KBr})_{1-x}(\text{KCN})_x$ system is not unique: a similar approach to the minimum thermal conductivity limit is observed in the $(\text{NaCl})_{1-x}(\text{NaCN})_x$ system; see Fig. 5. As the concentration of cyanide increases to $x \approx 0.10$, the thermal conductivity is decreased to Λ_{\min} near room temperature. At $x = 0.76$ the conductivity is glasslike over the full temperature range and only slightly smaller than for $x \approx 0.10$ at $T > 30$ K. As for $(\text{KBr})_{1-x}(\text{KCN})_x$, substitution of the oblong CN^- molecule on the halide site disrupts the crystalline lattice vibrations to a sufficient degree to produce a conductivity close to Λ_{\min} .

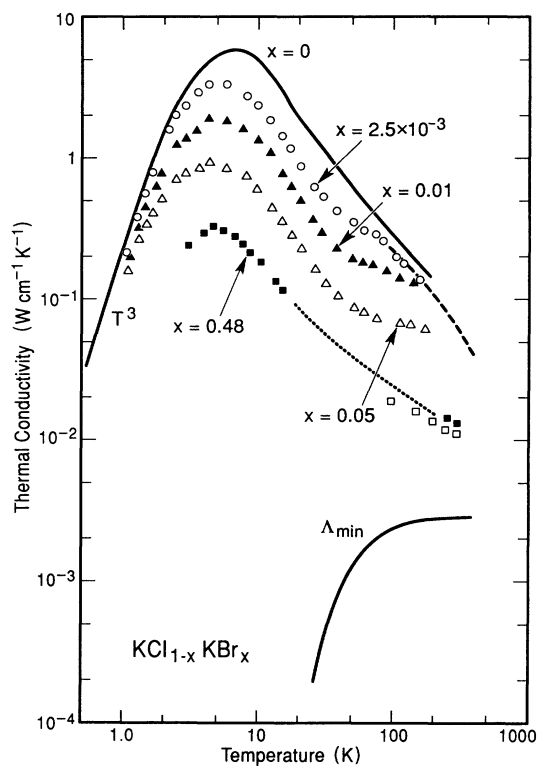


FIG. 3. Thermal conductivity of $\text{KCl}_{1-x}\text{Br}_x$. Data between 1 and 200 K for $0 < x \leq 0.05$ are by Baumann and Pohl (Ref. 33). Data for $x = 0.48$ were obtained from three investigations: see Williams (Ref. 43) for data (filled squares) below 20 K; open squares above 100 K are by Slack *et al.* (Ref. 44); two points near room temperature taken in this investigation by the 3ω are shown as filled squares. (The sample cracked during the measurement.) The solid line connecting the low- and high-temperature data for $x = 0.48$ is a guide to the eye. The dashed line is nominally pure KCl; see Ref. 44. The solid line marked Λ_{\min} is the calculated minimum thermal conductivity for pure KCl; see Ref. 2.

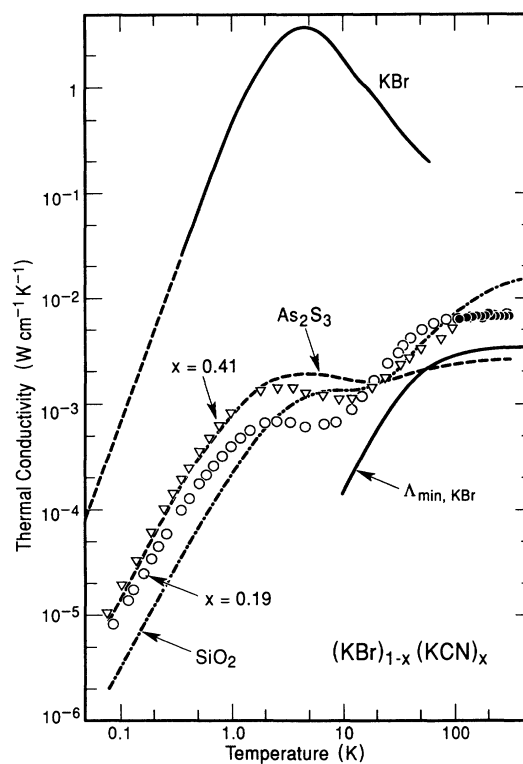


FIG. 4. Thermal conductivity of $(\text{KBr})_{1-x}(\text{KCN})_x$ for $x = 0$ (pure KBr), 0.19, and 0.41 compared to data for glasses and the calculated Λ_{\min} . Data for $x = 0.41$ at $T > 100$ K (solid circles) are nearly identical to data for $x = 0.19$ (open circles). Low-temperature data for $x = 0.19$ below 30 K and $x = 0.41$ below 100 K are from Ref. 26.

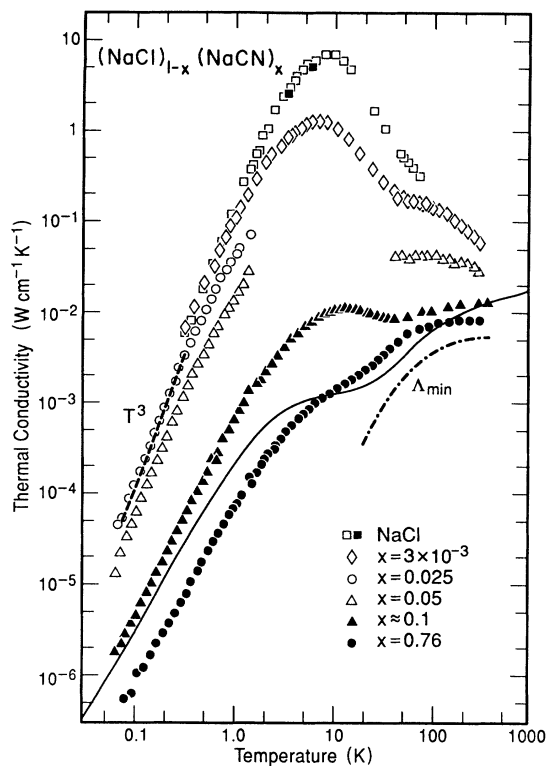


FIG. 5. Thermal conductivity of $(\text{NaCl})_{1-x}(\text{NaCN})_x$ mixed crystals and comparison to the calculated Λ_{\min} . The value of x refers to the composition of the crystal; the exact composition of the crystal marked $x \approx 0.10$ is somewhat uncertain; see text. NaCl and $x = 3 \times 10^{-3}$ data below 100 K; see Ref. 47. Solid squares for NaCl are from this investigation. The T^3 temperature dependence in the boundary scattering regime is shown by the dashed line. Data for $a\text{-SiO}_2$ (solid line) are included for comparison.

B. Fluorite structure crystals, $\text{Zr}_{1-x}\text{Y}_x\text{O}_{2-x/2}$ and $\text{Ba}_{1-x}\text{La}_x\text{F}_{2+x}$

The data discussed above show that simple monatomic substitution does not produce a glasslike conductivity at any temperature. Many fluorite structure crystals, on the other hand, accept large concentrations of substitutional atoms with different charge (producing either a large concentration of vacancies or interstitials), and this type of disorder *can* produce a glasslike conductivity. In $\text{Zr}_{1-x}\text{Y}_x\text{O}_{2-x/2}$ charge balance is maintained by vacancies with two Y^{+3} ions replacing two Zr^{+4} ions and leaving one oxygen vacancy; in $\text{Ba}_{1-x}\text{La}_x\text{F}_{2+x}$, each La^{+3} substitution for a Ba^{+2} adds an interstitial fluorine.²⁸

Walker and Anderson³⁸ studied low-energy excitations in crystals of $\text{Zr}_{1-x}\text{Y}_x\text{O}_{2-x/2}$, $0.18 < x < 0.30$, through low-temperature measurements of thermal conductivity, specific heat, thermal expansion, and dielectric loss. Although high-purity crystals are difficult to prepare because of the high melting point, single crystals with the cubic fluorite structure can be grown for $0.15 < x < 0.57$; below this range tetragonal and monoclinic structures make up the stable room-temperature phases. Low-temperature data³⁸ are plotted in Fig. 6 together with

data we obtained with the 3ω method.

The thermal conductivity is very similar to that of a glass and changes very little when x is almost doubled from $x = 0.15$ to 0.27 . This near independence on x shows that the conductivity has already reached its lower limit at $x = 0.15$. Unfortunately, single crystals cannot be made for $x < 0.13$, and the evolution of a glasslike conductivity cannot be observed free of scattering from grain boundaries and closely spaced twin planes. We are also unaware of data even for polycrystalline samples with $x < 0.10$ or data for pure ZrO_2 but see no reason why pure ZrO_2 should not have a thermal conductivity as is typical for all crystalline dielectrics.

Unlike $\text{Zr}_{1-x}\text{Y}_x\text{O}_{2-x/2}$, the fluorite structure of $\text{Ba}_{1-x}\text{La}_x\text{F}_{2+x}$ is stable at room temperature for all values of x between 0 and 0.50, and so a gradual transition from crystalline to glasslike conductivity is clearly demonstrated; see Fig. 7. The conductivity is reduced continuously as x is increased from 0 to 0.33. Increasing x from 0.33 to 0.46 does not change the conductivity near room temperature, where the data agree with the calcu-

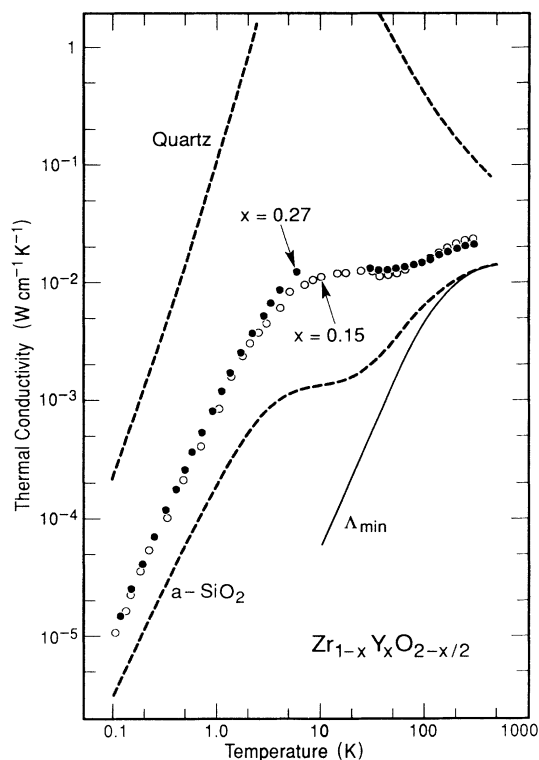


FIG. 6. Thermal conductivity of single crystal $\text{Zr}_{1-x}\text{Y}_x\text{O}_{2-x/2}$ with $x \approx 0.15$ (open circles) and $x \approx 0.30$ (filled circles). The exact concentrations are different in each set of data. Data below 5 K (Ref. 38) are for $x = 0.18$ (open circles) and $x = 0.30$ (solid circles). Between 5 and 30 K, $x = 0.13$ (open circles) obtained by Van Cleve (Ref. 57). Data above 30 K are from this investigation, $x = 0.15$ (open circles), and $x = 0.27$ (solid circles). The conductivity is almost independent of x and glasslike at all temperatures. The solid line is the calculated Λ_{\min} . Quartz and $a\text{-SiO}_2$ are shown for comparison.

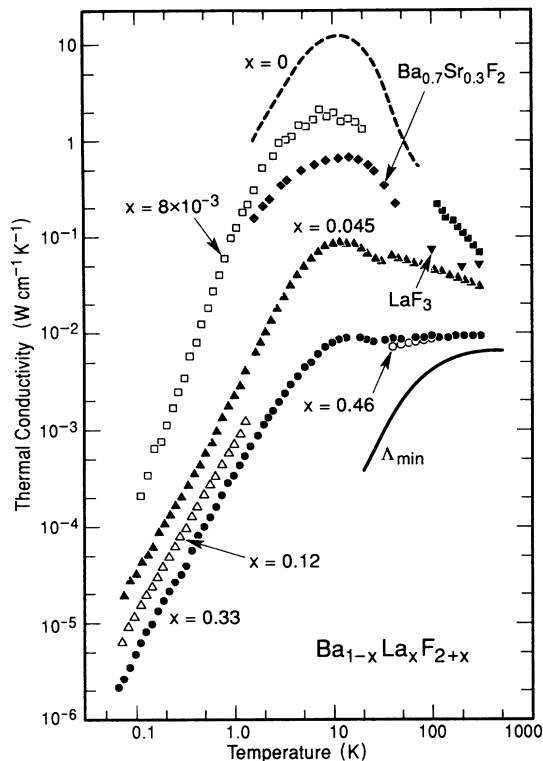


FIG. 7. Thermal conductivity of $\text{Ba}_{1-x}\text{La}_x\text{F}_{2+x}$. Data for $x = 0$ below 30 K (Ref. 45) are shown as a dashed line. Solid line is the calculated Λ_{\min} for BaF_2 . The $x = 0.46$ sample was not measured below 30 K because it was not as high quality as the other samples; see text.

lated Λ_{\min} (solid line); this is more evidence that the conductivity of a disordered crystal cannot be reduced below its minimum value. Glasslike thermal conductivity was also observed for a mixed crystal of nominal composition $\text{Ca}_{0.8}\text{La}_{0.2}\text{F}_{2.2}$,³⁹ demonstrating that this behavior is not confined to the $\text{Ba}_{1-x}\text{La}_x\text{F}_{2+x}$ system. A few scant data points for LaF_3 show that the conductivity returns to crystalline behavior at $x = 1$.⁴⁰

We also show in Fig. 7 data for $\text{Ba}_{0.7}\text{Sr}_{0.3}\text{F}_2$. These data again demonstrate that monatomic substitution (in this case Sr^{2+} on Ba^{2+} sites) is not sufficient to produce a glasslike conductivity.

C. Feldspars

Feldspars are three dimensionally linked crystals of aluminosilicates. Trivalent aluminum takes the place of four-valent silicon in the SiO_4 tetrahedron, and charge-balancing alkali (K,Na) and alkaline earth (Ca,Ba) ions occupy interstitial sites. The three important end members of the feldspar family are $\text{NaAlSi}_3\text{O}_8$ (albite, abbreviated Ab), KAlSi_3O_8 (orthoclase, Or), and $\text{CaAl}_2\text{Si}_2\text{O}_8$ (anorthite, An). They form a solid solution at all compositions $\text{Ab}_x\text{Or}_y\text{An}_z$, where x , y , and z are mole fractions. The distribution of the cations leads to the enormous and well-documented structural richness of the feldspars. Using the language we have been using for the mixed crystals in this paper, we talk about local distortions of

the framework structure resulting from the cation distributions on interstitial sites.

The extremely small thermal conductivity of feldspar minerals was first reported by Birch and Clark.¹⁰ In particular, in mixtures of the form $\text{Ab}_x\text{An}_{1-x}$, the plagioclase feldspars, phonon mean free paths of the order of the interatomic spacing, were observed near room temperature. In an extension of these measurements³¹ it was suggested that lamellar structures with spacings of the order of μm caused by compositional fluctuations in these feldspars might cause the extremely strong phonon scattering. However, it has since been shown by Linvill³⁰ that the same small thermal conductivity is also found in single-crystal feldspars in which such lamellar structures should be absent because of their thermal history. This work is reviewed below together with our measurements above 30 K.

In spite of their abundance in nature (feldspars con-

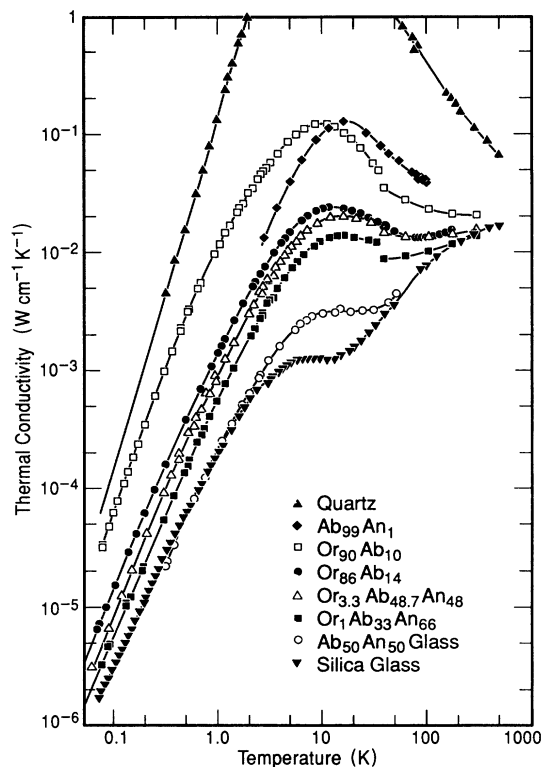


FIG. 8. Thermal conductivity of single-crystal feldspars, after Linvill (Ref. 30). Data above 30 K for $\text{Or}_{90}\text{Ab}_{10}$, $\text{Or}_{3.3}\text{Ab}_{48.7}\text{An}_{48}$, and $\text{Or}_1\text{Ab}_{33}\text{An}_{66}$ are from this investigation. According to specific-heat measurements (above 1 K) by Linvill (Ref. 30), the Debye specific heat of sanidine is $C_D = 1 \times 10^{-6} \text{ J g}^{-1} \text{ K}^{-4} \text{ T}^3$. From this, one determines a Debye velocity (Ref. 46) $v_D = 3.6 \times 10^5 \text{ cm sec}^{-1}$ and a thermal conductivity in the boundary regime $\Lambda_{\text{Casimir}} = 0.16 \text{ W cm}^{-1} \text{ K}^{-4} \text{ T}^3$, very close to that of α -quartz, $\Lambda = 0.14 \text{ W cm}^{-1} \text{ K}^{-4} \text{ T}^3$ for rod-shaped samples with 5-mm diameter. This similarity justifies the comparison of the conductivity of feldspars with that of α -quartz. Below $\sim 10 \text{ K}$, the conductivity of $\text{Ab}_{99}\text{An}_1$ is lowered because of scattering by internal structures resulting from chemical alterations.

stitute almost 60% of the Earth's crust⁴¹) single crystals of dimensions suitable for thermal conductivity measurements are extremely rare, and grain boundaries, macroscopic inclusions, and alterations tend to mask the phonon-scattering processes in the bulk below a few tens of degrees kelvin, thus limiting the usefulness of thermal conductivity measurements as a tool in a wide temperature range. Linvill succeeded in locating a number of nearly perfect single crystals of different compositions and thermal histories. Their thermal conductivities have been found to decrease with increasing chemical disorder; see Fig. 8. The comparison with the conductivity of pure crystal quartz is justified because of very similar speeds of sound, as explained in the figure caption. Note also that the conductivity of an amorphous sample of composition $\text{Ab}_{50}\text{An}_{50}$ agrees closely with that of amorphous SiO_2 .

The largest conductivity is found in the nearly pure

albite, of composition $\text{Ab}_{99}\text{An}_1$. This single crystal contains chemical alterations that probably result from water to which this sample had been exposed in its geologic environment. These alterations decrease the conductivity below 10 K through internal boundary scattering, as shown in Fig. 8. The smallest conductivity is observed on the feldspar of the composition $\text{Or}_1\text{Ab}_{33}\text{An}_{66}$, a labradorite. This sample had been cooled relatively rapidly, without undergoing any spinodal decomposition. The findings on this labradorite sample show that exsolution lamellae as caused by slow cooling and found in samples like the $\text{Or}_{3.3}\text{Ab}_{48.7}\text{An}_{48}$ cannot be the cause for the strong phonon scattering. Instead, we now conclude that the glasslike thermal conductivity in the feldspars arises predominantly from their chemical disorder. It is easy to envision that the random distribution of the Na^+ , K^+ , and Ca^{2+} ions in the feldspars leads to local distortions and thus to lattice vibrational properties very similar to

TABLE I. Parameters used to calculate the minimum thermal conductivity: n number density of atoms, and v_t and v_l transverse and longitudinal speeds of sound. Λ_{\min} is the minimum conductivity at 300 K calculated using Eq. (17). Λ_{meas} is the measured conductivity at that temperature.

	n 10^{22} cm^{-3}	v_t (km/s)	v_l (km/s)	Λ_{\min} (mW/cm K)	Λ_{meas} (mW/cm K)
Amorphous solids					
As_2S_3	3.92	1.44	2.65 ^a	3.45	2.46 ^b
Ca_3KNO_3	6.92	1.73	3.5 ^c	5.4	4.9 ^b
CdGeAs_2	4.11	1.86	3.03 ^d	4.31	3.90 ^d
Ge	4.41	2.63	4.35 ^d	6.21	5.05 ^d
Se	3.28	1.06	2.06 ^e	2.30	1.40 ^f
Si	5.00	4.37	7.36 ^d	9.9	10.5 ^g
SiO_2	6.63	3.74	5.98 ^h	10.4	12.4 ^b
Disordered crystals					
$\text{Ba}_{0.67}\text{La}_{0.33}\text{F}_{2.33}$	5.04	2.30	4.44 ⁱ	6.35	9.6 ^j
$\text{Ca}_{0.80}\text{La}_{0.20}\text{F}_{2.2}$	7.36	3.69	7.18 ^k	11.3	18.2 ^l
$(\text{KBr})_{0.81}(\text{KCN})_{0.19}$	2.81	1.68	3.03 ^m	3.19	6.7 ^j
$(\text{NaCl})_{0.24}(\text{NaCN})_{0.76}$	4.46	2.44	4.75 ⁿ	6.4	9.0 ^j
$\text{Or}_1\text{Ab}_{33}\text{An}_{66}$	7.76	2.8	5.6 ^o	9.8	13.6 ^j
YB_{66}	13.8	7.9	12.0 ^p	18.6	25.5 ^q
$\text{Zr}_{0.85}\text{Y}_{0.15}\text{O}_{1.925}$	8.41	3.86	7.6 ^r	12.5	23.8 ^j

^aR. B. Stephens (private communication).

^bReference 23.

^cJ. J. De Yoreo, Ph.D. thesis, Cornell University, 1985 (unpublished).

^dDavid G. Cahill and R. O. Pohl, Phys. Rev. B **37**, 8773 (1988).

^eJ. C. Lasjaunias *et al.*, Solid State Commun. **10**, 215 (1972).

^fReference 2.

^gReference 7.

^hW. F. Love, Phys. Rev. Lett. **31**, 822 (1973).

ⁱDavid G. Cahill, Ph.D. thesis, Cornell University, 1989 (unpublished).

^jThis investigation.

^kD. R. Huffman and M. H. Norwood, Phys. Rev. **117**, 709 (1960).

^lReference 39.

^mReference 25.

ⁿJ. T. Lewis, A. Lehoczy, and C. V. Briscoe, Phys. Rev. **161**, 877 (1967).

^oReference 30.

^pG. A. Slack, D. W. Oliver, G. D. Brower, and J. D. Young, J. Phys. Chem. Solids **38**, 45 (1977).

^qReference 16.

^rReference 29.

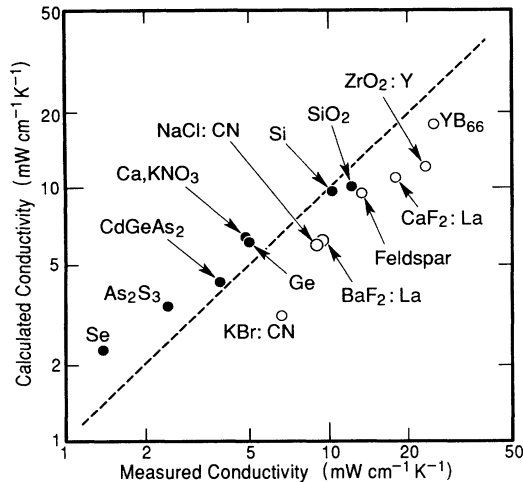


FIG. 9. Composite plot of the calculated minimum conductivity at 300 K vs the measured values; perfect agreement is shown by the dashed line. Amorphous solids are shown as filled circles and disordered crystals as open circles. The atomic densities and speeds of sound used to calculate Λ_{\min} are listed in Table I.

those produced in the mixed crystals described above.

Finally, we note that even for the most disordered (crystalline) feldspar the thermal conductivity still is considerably larger than that of the amorphous $\text{Ab}_{50}\text{An}_{50}$ at

$T < 100$ K. This comparison emphasizes the importance of referring to the lattice vibrations of these disordered crystals as "glasslike." They are, as shown in the example, not identical to those of the amorphous phase. In this context, we refer to a recent study regarding the thermal conductivity¹⁵ and the tunneling states⁴² in glass-ceramics.

V. CONCLUSION

As summarized in Fig. 9 and Table I, Eq. (17), which is based on Einstein's model, is an accurate predictor of the conductivity of a wide range of amorphous solids and highly disordered crystals. Also, we have been unable to produce an example of a disordered solid that has a conductivity significantly below Λ_{\min} and conclude that the concept of a minimum thermal conductivity is valid. Disorder produced by simple monatomic substitution cannot lead to glasslike lattice vibrations. The existence of glasslike lattice vibrations in a disordered crystal appears to be linked to the presence of random, noncentral distortions of the lattice.

ACKNOWLEDGMENTS

This work was supported by the U.S. National Science Foundation, Grant No. DMR-87-14-788, and the Cornell Materials Science Center. One of us (S.K.W.) thanks the TRW Corporation for financial support.

¹David G. Cahill and R. O. Pohl, *Annu. Rev. Phys. Chem.* **39**, 93 (1988).

²David G. Cahill and R. O. Pohl, *Solid State Commun.* **70**, 927 (1989).

³A. Einstein, *Ann. Phys.* **35**, 679 (1911).

⁴G. A. Slack, in *Solid State Physics*, edited by F. Seitz and D. Turnbull (Academic, New York, 1979), Vol. 34, p. 1; see in particular p. 57.

⁵R. Orbach, *Philos. Mag.* **B 65**, 289 (1992).

⁶Philip B. Allen and Joseph L. Feldman, *Phys. Rev. Lett.* **62**, 645 (1989).

⁷David G. Cahill, Henry E. Fischer, Tom Klitsner, E. T. Swartz, and R. O. Pohl, *J. Vac. Sci. Technol. A* **7**, 1259 (1989).

⁸P. Sheng and M. Y. Zhou, *Science* **253**, 539 (1991).

⁹Y. H. Lee, R. Biswas, C. M. Soukoulis, C. Z. Wang, C. T. Chan, and K. M. Ho, *Phys. Rev. B* **43**, 6573 (1991).

¹⁰F. Birch and H. Clark, *Am. J. Sci.* **238**, 529 (1940).

¹¹A. C. Anderson, *Phase Trans.* **5**, 301 (1985).

¹²R. O. Pohl, J. J. De Yoreo, M. Meissner, and W. Knaak, in *Physics of Disordered Materials*, edited by D. Adler, H. Fritzsche, and S. Ovshinsky (Plenum, New York, 1985), p. 529.

¹³W. N. Lawless and S. L. Swartz, *Phys. Rev. B* **28**, 2125 (1983).

¹⁴J. J. De Yoreo, R. O. Pohl, and Gerald Burns, *Phys. Rev. B* **32**, 5780 (1985).

¹⁵David G. Cahill, J. R. Olson, Henry E. Fischer, S. K. Watson, R. B. Stephens, R. H. Tait, T. Ashworth, and R. O.

Pohl, *Phys. Rev. B* **44**, 12226 (1991).

¹⁶David G. Cahill, Henry E. Fischer, S. K. Watson, R. O. Pohl, and G. A. Slack, *Phys. Rev. B* **40**, 3254 (1989).

¹⁷A. Eucken, *Ann. Phys.* **35**, 185 (1911).

¹⁸A. Einstein, *Ann. Phys.* **22**, 180 (1907).

¹⁹David G. Cahill, *Rev. Sci. Instrum.* **61**, 802 (1990).

²⁰To the best of our knowledge, the first report in the scientific literature of a third harmonic detection scheme in thermal measurement is by S. R. Atalla, A. A. El-Sharkawy, and F. A. Gasser, *Int. J. Thermophys.* **2**, 155 (1981). Interestingly, the detection of flaws in circuit board wiring using harmonic generation was patented more than 20 years ago; for a recent review of the relevant patents see T. H. Di Stefano and A. Halperin, U. S. Patent No. 4,496,900, Jan. 29, 1985.

²¹N. O. Birge and S. R. Nagel, *Phys. Rev. Lett.* **54**, 2674 (1985).

²²N. O. Birge and S. R. Nagel, *Rev. Sci. Instrum.* **58**, 1464 (1987).

²³For a brief review of related "hot-wire" techniques, see David G. Cahill and R. O. Pohl, *Phys. Rev. B* **35**, 4067 (1987).

²⁴A. V. Karlsson, *Phys. Rev. B* **2**, 3332 (1970).

²⁵Susan K. Watson, David G. Cahill, and R. O. Pohl, *Phys. Rev. B* **40**, 6381 (1989).

²⁶J. J. De Yoreo, W. Knaak, M. Meissner, and R. O. Pohl, *Phys. Rev. B* **34**, 8828 (1986).

²⁷S. Elschner, K. Knorr, and A. Loidl, *Z. Phys. B* **61**, 209 (1985).

- ²⁸David G. Cahill and R. O. Pohl, *Phys. Rev. B* **39**, 10477 (1989).
- ²⁹H. M. Kandil, J. D. Greiner, J. F. Smith, *J. Am. Ceram. Soc.* **67**, 541 (1984).
- ³⁰M. L. Linvill, Ph.D. thesis, Cornell University, 1987 (unpublished).
- ³¹R. O. Pohl and J. W. Vandersande, *Materials Research Society Symposium Proceedings*, edited by D. G. Brookins (Elsevier, New York, 1983), Vol. 15, p. 711; M. L. Linvill, J. W. Vandersande, and R. O. Pohl, *Bull. Mineral.* **107**, 521 (1984); M. L. Linvill and R. O. Pohl, in *Thermal Conductivity 18*, edited by T. Ashworth and D. R. Smith (Plenum, New York, 1985), p. 653.
- ³²A. Eucken and E. Kuhn, *Z. Phys. Chem.* **134**, 193 (1928); these data are discussed by W. D. Kingery and M. C. McQuarrie, *Am. Ceram. Soc.* **37**, 68 (1954).
- ³³F. C. Baumann and R. O. Pohl, *Phys. Rev.* **163**, 843 (1967).
- ³⁴B. D. Nathan, L. F. Lou, and R. H. Tait, *Solid State Commun.* **19**, 615 (1976).
- ³⁵B. Abeles, D. S. Beers, G. D. Cody, and J. P. Dismukes, *Phys. Rev.* **125**, 44 (1962); E. F. Steigmeir, B. Abeles, and R. M. Miller, *J. Appl. Phys.* **36**, 76 (1965).
- ³⁶J. J. De Yoreo, M. Meissner, R. O. Pohl, R. M. Rowe, J. J. Rush, and S. Susman, *Phys. Rev. Lett.* **51**, 1050 (1983).
- ³⁷Eric R. Grannan, Mohit Randeria, and James P. Sethna, *Phys. Rev. Lett.* **60**, 1402 (1988).
- ³⁸F. J. Walker and A. C. Anderson, *Phys. Rev. B* **29**, 5881 (1984).
- ³⁹David G. Cahill and R. O. Pohl, in *Materials Research Society Symposium Proceedings*, edited by D. D. Allred, C. B. Vining, and G. A. Slack (MRS, Pittsburgh, 1991), Vol. 234, p. 27.
- ⁴⁰Phillip H. Klein and William J. Croft, *J. Appl. Phys.* **38**, 1603 (1967); these data for LaF_3 were obtained on crystals that were "visibly clouded by the presence of lanthanum oxide and oxyfluoride."
- ⁴¹K. C. Condie, *Plate Tectonics and Crustal Evolution* (Pergamon, New York, 1982).
- ⁴²A. K. Raychaudhuri and R. O. Pohl, *Phys. Rev. B* **44**, 12233 (1991).
- ⁴³Wendell S. Williams, *Phys. Rev.* **119**, 1021 (1960).
- ⁴⁴G. A. Slack, P. Andersson, and R. Ross (unpublished).
- ⁴⁵James A. Harrington and Charles T. Walker, *Phys. Rev. B* **1**, 882 (1970).
- ⁴⁶J. V. Smith, *Feldspar Minerals*, Vol. 1 of *Crystal Structure and Physical Properties* (Springer-Verlag, Berlin, 1974).
- ⁴⁷W. D. Seward and V. Narayanamurti, *Phys. Rev.* **148**, 463 (1966).